



The Mid-UV Spectrum of Irradiated NaCl at Europa-like Conditions

Michael E. Brown¹, William T. P. Denman¹, and Samantha K. Trumbo¹Division of Geological and Planetary Sciences, California Institute of Technology, Pasadena, CA 91125, USA; mbrown@caltech.edu

Received 2021 July 30; revised 2021 December 3; accepted 2021 December 21; published 2022 February 2

Abstract

Recent observations from the Hubble Space Telescope show a mid-UV absorption feature localized to leading-hemisphere chaos regions on Europa. The same regions were previously found to have a visible absorption at 450 nm that was attributed to the presence of irradiated NaCl. The lack of any additional diagnostic absorptions for NaCl in the visible spectrum of these terrains made confirmation of this identification difficult. Here we use laboratory experiments to show that NaCl irradiated at Europa's surface temperatures develops an absorption at ~220 nm, consistent with the new detection in Europa's mid-UV spectrum, strongly supporting the NaCl identification. Irradiated NaCl in leading-hemisphere chaos terrain would suggest that sodium and chlorine are important components of Europa's subsurface ocean.

Unified Astronomy Thesaurus concepts: [Europa \(2189\)](#); [Surface composition \(2115\)](#); [Laboratory astrophysics \(2004\)](#); [Ultraviolet astronomy \(1736\)](#)

1. Introduction

Jupiter's satellite Europa has an icy surface that shows spectroscopic evidence for the presence of salts, particularly in the regions that appear to have been most recently geologically resurfaced (McCord et al. 1999). These salts are likely ultimately derived from the large interior ocean of Europa and thus record information on the composition of this ocean. Most of the information on the composition of these salts has come from near-infrared spectroscopy. Unfortunately, the near-infrared spectra of Europa are ambiguous: distorted water ice bands indicative of hydrated minerals are clearly present, but few diagnostic spectral bands are present that would allow unique identification of the salts.

Owing to these difficulties, three major interpretations for the native salt composition of the surface of Europa have been proposed. Galileo NIMS data were largely interpreted as showing the presence of magnesium sulfate salts as well as radiolytically produced sulfuric acid on the sulfur-bombarded trailing hemisphere (McCord et al. 1998; Carlson et al. 1999; Dalton et al. 2005; Shirley et al. 2010; Dalton et al. 2012). Ground-based observations from the Keck Observatory at higher spectral resolution confirmed the presence of sulfuric acid on the trailing hemisphere, but failed to detect any of the distinctive spectral features expected from magnesium sulfates on most of the surface, leading to the hypothesis of a native salt composition dominated by spectrally bland sodium chloride, with the sodium chloride dominating leading-hemisphere chaos regions (Brown & Hand 2013; Fischer et al. 2015). Though subsequent observations from the Very Large Telescope did not detect any additional spectral features, they were modeled as a combination of (presumably native) magnesium chloride salt as well as (presumably radiolytic) magnesium chlorates, magnesium perchlorates, and sulfuric acid (Ligier et al. 2016), with the chloride salts dominating on the trailing, rather than leading side in this model. With few spectral features in the

near-infrared on which to base these interpretations, resolution of this compositional ambiguity is difficult.

Pure chloride salts tend to be spectrally featureless in the visible wavelength region, but irradiation can change these characteristics. Irradiated sodium chloride, in particular, grows spectral absorption features owing to the presence of electrons occupying lattice locations vacated by chlorine ions (Seitz 1946). Hand & Carlson (2015) and Poston et al. (2017) studied these visible absorptions—called “color centers”—at Europa-like conditions and showed the presence of a broad 460 nm absorption (called an “F-center”) due to these electrons as well as an absorption at 720 nm (an “M-center”) due to physically adjacent pairs of F-centers. Observations from the Hubble Space Telescope (HST) showed a distinct absorption feature at 450 nm, interpreted to be F-center absorption, but no hint of the expected M-center absorption at 720 nm. Trumbo et al. (2019) hypothesized that a balance between radiolytical F-center production and photobleaching—the destruction of F-centers by photoexcitation of the trapped electrons—led to a low equilibrium number of F-centers too small to ever have sufficient numbers of adjacent pairs to begin to form M-centers. This hypothesis was confirmed by Denman et al. (2022), who showed that more carefully controlled temperatures led to F-centers shifted to the HST-observed 450 nm wavelengths and that solar-like illumination conditions can lead to the presence of an F-center with no M-centers, matching the Europa observations.

Recently, Trumbo et al. (2022) detected a second spectral absorption in the same leading-hemisphere chaos regions where the absorption attributed to the NaCl F-center was detected. This new mid-ultraviolet (UV) feature, with a central wavelength of approximately 230 nm, occurs near the reported wavelength of the V₃ color center in NaCl, a feature that occurs due the displacement of Cl atoms from their normal lattice positions and the subsequent formation of Cl₃⁻¹ molecular ions in nearby Cl lattice sites (Alexander & Schneider 1950; Casler et al. 1950; Schwartz et al. 2008). V₃ centers are stable up to ~500K and have a poorly determined central absorption wavelength near 210 nm. The UV spectra could also be affected by the presence of H-centers with an absorption near 330 nm, which are caused by Cl₂⁻¹ molecular locations in Cl lattice sites but which are thought to be unstable at



Original content from this work may be used under the terms of the [Creative Commons Attribution 4.0 licence](#). Any further distribution of this work must maintain attribution to the author(s) and the title of the work, journal citation and DOI.

temperatures above about 80 K (Schwartz et al. 2008). These features have never been studied at the temperatures of the surface of Europa or in reflection spectroscopy, making comparison to the HST data difficult. Here we measure the mid-UV spectrum of irradiated NaCl at Europa-like conditions from 200 to 700 nm to allow for direct comparison to the HST spectra of Trumbo et al. (2022).

2. Experimental Setup

The experimental setup for observing irradiated NaCl is described in detail in Denman et al. (2022). In short, we irradiate $\sim 500 \mu\text{m}$ NaCl grains with 10 keV electrons in a 16 cm diameter vacuum chamber kept at a pressure of 1×10^{-8} torr and at controllable temperatures. To ensure thermal coupling between the salt grains and the cold finger, the grains are pressed into indium foil inside of the sample holder and any excess grains are poured off. The temperatures we report are of the cold finger itself, so even with the indium foil the sample temperature could still be somewhat elevated above this temperature. Because of this procedure, small amounts of indium are visible in the sample cup, but our calibration ensures that the visibility of indium does not affect the final results, and we have verified that irradiating indium with electrons at the same dosage level used here does not change its mid-UV spectrum by more than $\sim 2\%$.

To obtain spectra, we illuminate the sample with a stabilized deuterium UV lamp at a 45° angle to the sample, and, to obtain a diffuse reflection, we observe at an angle 90° away from the specular beam. The beam illuminates only the sample inside the holder, ensuring that all observed light comes from the sample. The diffusely reflected beam is fed into a fiber-coupled spectrometer which obtains a 200–1100 nm spectrum in a single exposure. To maximize the signal-to-noise down to a 200 nm, where little light from the lamp is created, we collect long exposures and allow the spectrum to saturate in some lamp emission features redward of 500 nm. In the data analysis, we extrapolate over these saturated regions.

Within the chamber, relative reflectance calibration is obtained with respect to the unirradiated NaCl. We calibrate the absolute reflectance of the NaCl exterior to the chamber by comparing to the spectrum of PTFE powder freshly pressed to a density of 1.025 g cm^{-3} , which is essentially uniform except for a $\sim 2\%$ decline in reflectance from 500 nm to 200 nm (Weidner & Hsia 1981). Comparison of the PTFE to a full NaCl sample (with no indium foil showing) shows that NaCl is nearly uniformly reflective across the UV–visible, but that a small absorption begins blueward of 240 nm. Experimentation with grinding the NaCl grains to smaller sizes shows that these features become smaller and should be essentially unobservable at the tens of microns sizes of the particles thought to be on Europa (McCord et al. 1998). For the remainder of our analysis we will therefore assume that unirradiated NaCl is spectrally uniform across our wavelength range, and we will reference all of our spectra to that of the cold unirradiated NaCl in vacuum.

The spectrum of NaCl within the chamber will contain small amounts of contamination from the spectrum of indium, which is marginally visible between NaCl grains. As we are referencing the unirradiated sample, the spectral contamination will be removed by the reference, unless the indium changes when irradiated. To ensure that the indium does not influence the spectral results, we irradiated pure indium foil at the full dosage of the experiments described below. No spectral changes were

found at the $\sim 1.5\%$ level (see Appendix). In addition, we performed room temperature NaCl irradiation experiments with no indium, and, while the growth rate and central wavelength of the spectral features change due to the higher temperatures, all of the spectral features seen in the experiments described below with indium are reproduced. We are thus confident that the spectral changes seen are due to changes in the NaCl.

We perform two series of experiments, bracketing the expected 120 K day-side and 80 K night-side temperature of the Europa equator. In both experiments we irradiate the grains with a current density of 12 nA cm^{-2} . Assuming a $1.2 \mu\text{m}$ penetration depth for these 10 keV electrons (Poston et al. 2017), this current density provides ~ 250 times the energy flux as received at the top $1.2 \mu\text{m}$ of the surface of Europa. Denman et al. (2022) showed the importance of photobleaching during irradiation in reaching an equilibrium between F-center creation and destruction. Our UV lamp provides little illumination at the 450 nm wavelength of the F-center, so, when not obtaining spectra, we switch on the visible spectral lamp, which provides approximately 13 times less than the noon-time equatorial solar irradiation at Europa. Because of the mismatch between the amount of irradiation and the amount of photobleaching, we do not reach equilibrium and F-centers continue to grow. We thus terminate our experiments when the features are fully developed but before saturation.

3. Results

The results of irradiation at 80 K and at 120 K are shown in Figure 1. In both cases, a well-defined F-center at 450 nm develops within the first 15 minutes, and a weaker band in the mid-UV begins to appear. At our low-dose levels, M-centers at 720 nm never appear. Small differences between the 80 K and 120 K irradiation are apparent. The 80 K irradiation develops a broad band from 300 to 400 nm on the shoulder of the F-center band that is not apparent in the 120 K radiation, and at 80 K the F-center grows more slowly and is slightly shifted blueward. The mid-UV band of the 80 K irradiation is initially shifted redward with respect to 120 K, but by the end of the irradiation the mid-UV feature at 80 K and 120 K appears identical. The absorption from 300 to 400 nm is likely due to the presence of H-centers in the colder sample. These defects become unstable at temperatures above ~ 80 K and recombine with F-center defects (Schwartz et al. 2008). The change in the F-center wavelength with temperature has been previously noted (Schwartz et al. 2008, Denman et al. 2022).

To further explore the effects of temperature and of photobleaching, we terminated the electron irradiation and warmed the 80 K sample to 120 K. After 2 hr of photobleaching the UV feature remains unchanged while the F-center has shifted redward and begun to decay. The H-center absorption appears to be gone completely (Figure 2).

Given that the ratio of photobleaching to irradiation experienced by Europa is significantly higher than in our experiments, it is plausible that this last spectrum could best represent the surface conditions of Europa, with 80 K irradiation at night allowing color centers to grow and then 120 K temperatures with intense photobleaching during the day to causing them to decay back away. The difference in decay rate between the photobleached V_3 and F-centers and the likely difference between the photon and electron penetration depth suggests that at equilibrium the ratio of the features could differ from that seen in our experiments.

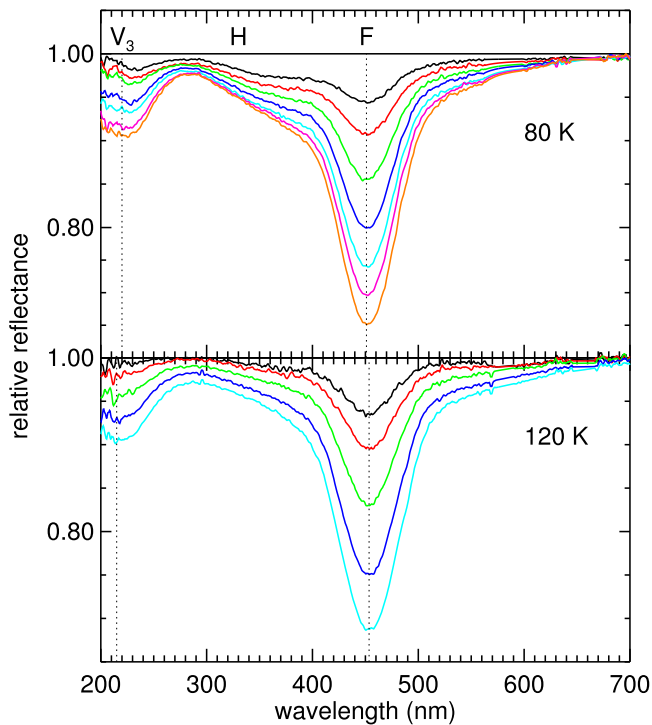


Figure 1. The spectrum of NaCl irradiated at 80 and 120 K with 10 keV electrons. Spectra are shown relative to the spectrum of unirradiated NaCl, which is expected to be nearly spectrally flat through this region. The irradiation times are 15 minutes (black), 30 minutes (red), 1 hr (green), 2 hr (blue), 3 hr (turquoise), 4 hr (magenta), and 5 hr (orange). For the 80 K irradiation, dashed lines at 220 and 451 nm show the central wavelengths of the color centers, while at 120 K these shift to 453 and 215 nm.

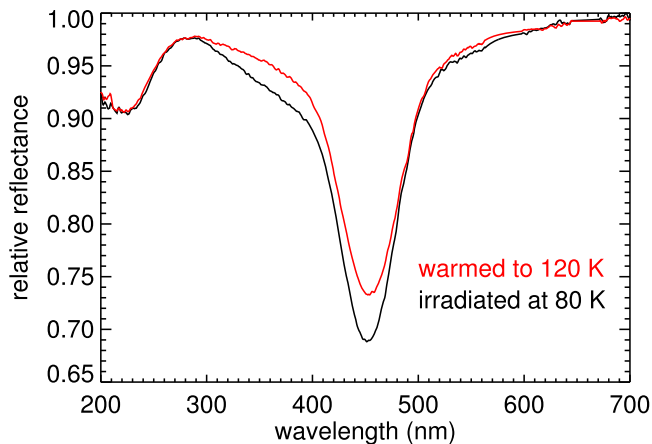


Figure 2. NaCl irradiated at 80 K for 5 hr (black) compared to the same sample after termination of radiation, raising of the temperature to 120 K, and photobleaching at Europa-like fluxes for 2 hr. The F-center absorption decays and shifts redward with higher temperatures and photobleaching, the H-center absorption appears to dissipate entirely, and the V_3 absorption remains unchanged.

4. Implications for Europa

NaCl irradiated at the temperatures of the surface of Europa develops an absorption band from <200 to 280 nm which is broadly consistent with the feature detected from HST spectroscopy on Europa (Trumbo et al. 2022). This V_3 color center and the F color center at 450 nm are the only distinct absorption features seen in our experiments. The HST results show that the UV absorption and the 450 nm absorption are

spatially coincident, localized to leading-hemisphere chaos regions. These results, along with the photobleaching experiments showing that M-center absorption at 720 nm should not be expected on Europa (Denman et al. 2022), support a consistent conclusion that irradiated NaCl is present in the leading-hemisphere chaos terrains of Europa.

NaCl on Europa is unlikely to be exogenic. Though NaCl is present in the Jupiter system owing to a source on Io (Lellouch et al. 2003), the spatial segregation of the NaCl to specific geographic regions is difficult to explain unless the NaCl is endogenic to Europa. Geologically young chaos terrains are a natural location to find salts recently sourced from the interior. While the chaos terrains may not directly sample ocean water, their endogenic composition must nonetheless be controlled by subsurface chemistry.

In the simple slow-freezing framework and experiments of Johnson et al. (2019), the presence of NaCl suggests the freezing of a sodium- and chlorine-rich, but relatively sulfate-poor, brine. In such a case, abundant sulfate salts on the surface would come from sulfur bombardment and would presumably be concentrated on the trailing hemisphere similarly to the radiolytically produced sulfuric acid (Carlson et al. 1999; Fischer et al. 2015). $MgCl_2$ salts, as proposed by Ligier et al. (2016), could also freeze from such brines if the Mg content is sufficiently high. Radiolytic or photolytic processing could then yield perchlorides and perchlorates of magnesium (Johnson et al. 2019), though their proposed spatial distribution on Europa would be difficult to explain. The attempt to determine the surface composition of Europa using linear spectral modeling of Ligier et al. (2016) ruled out NaCl in favor of these Mg-bearing chlorinated salts. The detection of two distinct spectral features consistent with those expected from irradiated NaCl perhaps highlights the difficulties of using such modeling to infer detailed surface composition. With distinct spectral features expected from NaCl now firmly detected, reliably determining the presence or absence of chlorinated magnesium salts and of sulfates would be a major step forward in understanding the chemistry of the ocean of Europa and the radiolytic processing that occurs on its surface.

This research was supported by a grant No. 668346 from the Simons Foundation.

Appendix

Sodium chloride crystals pressed into indium foil provide significantly better thermal coupling than when the crystals are simply sitting on a cold finger (Denman et al. 2022). In our experiments, we press the crystals into the foil and pour off any crystals which are not sufficiently embedded into the foil to stick. Such a process leaves a sample which is nearly completely covered in crystals, but through which the indium can be seen through a small fraction of the surface area (Figure A1). To ensure that the changes that were observed in our sample upon irradiation were due solely to effects in the sodium chloride, we are irradiating bare indium to search for any radiation-induced changes. Reproducing the same flux and dosage as the sodium chloride experiments, we find changes of no more than $\pm 1.5\%$ in the indium (Figure A2). These very small changes, coupled with the small fraction of indium visible, ensure that all changes seen in the spectra are due to sodium chloride.



Figure A1. The sodium chloride sample after pressing into indium foil and pouring off nonattached grains. The surface area of the sample predominantly shows sodium chloride grains, though in the specular image on the right reflection can be seen from some small regions of bare indium.

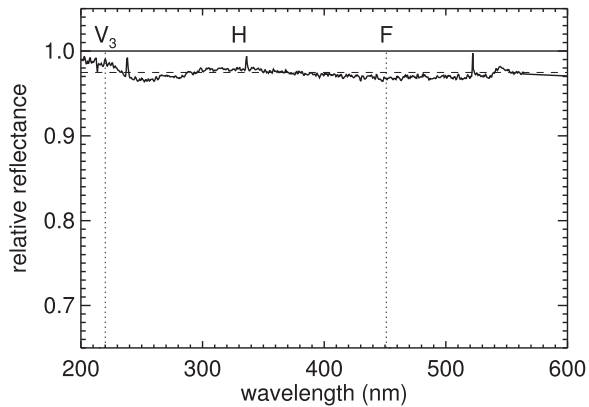


Figure A2. A spectrum of pure indium foil irradiated for 3 hours at identical conditions to the NaCl experiments divided by the spectrum of unirradiated indium (equivalent to the turquoise-colored curves in Figure 1). Irradiation of indium causes no features larger than $\pm 1.5\%$ to appear in the reflectance spectrum.

ORCID iDs

Michael E. Brown <https://orcid.org/0000-0002-8255-0545>
 William T. P. Denman <https://orcid.org/0000-0003-4752-0073>
 Samantha K. Trumbo <https://orcid.org/0000-0002-0767-8901>

References

- Alexander, J., & Schneider, E. 1950, *Natur*, **164**, 653
 Brown, M. E., & Hand, K. P. 2013, *AJ*, **145**, 110
 Carlson, R. W., Johnson, R. E., & Anderson, M. S. 1999, *Sci*, **286**, 97
 Casler, R., Pringsheim, P., & Yuster, P. 1950, *JChPh*, **18**, 1564
 Dalton, J. B., Prieto-Ballesteros, O., Kargel, J. S., et al. 2005, *Icar*, **177**, 472
 Dalton, J. B., Shirley, I., & Kamp, L. W., J. H. 2012, *JGRE*, **117**, E03003
 Denman, W. T. P., Trumbo, S. K., & Brown, M. E. 2022, *PSJ*, **3**, 26
 Fischer, P. D., Brown, M. E., & Hand, K. P. 2015, *AJ*, **150**, 164
 Hand, K. P., & Carlson, R. W. 2015, *GeoRL*, **42**, 3174
 Johnson, P. V., Hodyss, R., Vu, T. H., & Choukroun, M. 2019, *Icar*, **321**, 857
 Lellouch, E., Paubert, G., Moses, J. I., Schneider, N. M., & Strobel, D. F. 2003, *Natur*, **421**, 45
 Ligier, N., Poulet, F., Carter, J., Brunetto, R., & Gourgeot, F. 2016, *AJ*, **151**, 163
 McCord, T. B., Hansen, G. B., Fanale, F. P., et al. 1998, *Sci*, **280**, 1242
 McCord, T. B., Hansen, G. B., Matson, D. L., et al. 1999, *JGR*, **104**, 11827
 Poston, M. J., Carlson, R. W., & Hand, K. P. 2017, *JGRE*, **122**, 2644
 Schwartz, K., Volkov, A. E., Sorokin, M. V., et al. 2008, *PhRvB*, **78**, 024120
 Seitz, F. 1946, *RvMP*, **18**, 384
 Shirley, J. H., Dalton, J. B., Prockter, L. M., & Kamp, L. W. 2010, *Icar*, **210**, 358
 Trumbo, S. K., Becker, T. M., Brown, M. E., Denman, W. T. P., & Molyneux, P. 2022, *PSJ*, **3**, 27
 Trumbo, S. K., Brown, M. E., & Hand, K. P. 2019, *SciA*, **5**, aaw7123
 Weidner, V., & Hsia, J. 1981, *JOSA*, **71**, 856